Clin. Lab. 2024;70:XXX-XXX

ORIGINAL ARTICLE

Identifying Hub Genes Related to Vascular Endothelial Cell Permeability Through Bioinformatics and Verification

Yunjiang Zheng, Qianyi Chen, Lei Cao, Lili Zhao, Yi Tang, Zhihan Liu

Department of Critical Care Medicine, Chongming Hospital Affiliated to Shanghai University of Medicine and Health Sciences, Chongming, Shanghai, China

SUMMARY

Background: **In this study, we aimed to identify the hub genes responsible for increased vascular endothelial cell permeability.**
Methods: **We applied the weighted Gene Expression Omnibus (GEO) database to mine dataset GSE178331 and obtained the most relevant high-throughput sequenced genes for an increased permeability of vascular endothelial cells due to inflammation. We constructed two weighted gene co-expression network analysis (WGCNA) networks, and the differential expression of high-throughput sequenced genes related to endothelial cell permeability were screened from the GEO database. Gene Ontology (GO) and Kyoto Encyclopedia of Genes and Genomes (KEGG) enrichment analysis were performed on the differential genes. Their degree values were obtained from the topological properties of protein-protein interaction (PPI) networks of differential genes, and the hub genes associated with an increased endothelial cell permeability were analyzed. Reverse transcription-polymerase chain reaction (RT-PCR) and western blotting techniques were used to detect the presence of these hub genes in TNF-α induced mRNA and the protein expression in endothelial cells.**
Results: **In total, 1,475 differential genes were mainly enriched in the cell adhesion and TNF-α signaling pathway. With TNF-α inducing an increase in the endothelial cell permeability and significantly increasing mRNA and protein expression levels, we identified three hub genes, namely PTGS2, ICAM1, and SNAI1. There was a significant difference in the high-dose TNF-α group and in the low-dose TNF-α group compared to the control group, in the endothelial cell permeability experiment ($p = 0.008$ vs. $p = 0.02$). Measurement of mRNA and protein levels of PTGS2, ICAM1, and SNAI1 by western blotting analysis showed that there was a significant impact on TNF-α and that there was a significant dose-dependent relationship ($p < 0.05$ vs. $p < 0.01$).**
Conclusions: **The three hub genes identified through bioinformatics analyses in the present study may serve as biomarkers of increased vascular endothelial cell permeability. The findings offer valuable insights into the progress and mechanism of vascular endothelial cell permeability.**
(Clin. Lab. 2024;70:xx-xx. DOI: 10.7754/Clin.Lab.2024.231125)

Correspondence:
Qianyi Chen, PhD
Department of Critical Care Medicine
Chongming Hospital Affiliated to Shanghai University of Medicine and Health Sciences
No. 25 Nanmen Road
Chengqiao Town, Chongming District
Shanghai, 202150
China
Phone: + 86 2169692110
Fax: + 862169691066
Email: qianyichencqy@outlook.com

Manuscript accepted January 31, 2024

KEYWORDS

endothelial cells, hub gene, permeability, weighted gene co-expression network analysis, verification

INTRODUCTION

Endothelial cells (ECs) have a barrier function, and under normal circumstances, this barrier function can prevent the leakage of large molecules inside the blood vessels to the outside. However, when ECs are damaged

by inflammation, toxins, ischemia, and hypoxia, they are activated and the integrity of the endothelial barrier function is disrupted. Studies have shown that an increased permeability of ECs is the basis of capillary leakage [1,2], which is a common occurrence. Medical conditions such as sepsis, acute lung injury, severe acute pancreatitis, trauma, infection, inflammation, and so on are accompanied by capillary leakage. Therefore, in a sense, where there is inflammation, there is leakage [3-6]. The leakage of macromolecular substances in blood vessels through endothelial cell gaps leads to intercellular edema, increases intercellular distance, and causes cell hypoxia. A large amount of inflammatory cytokines accumulates in local tissues, leading to tissue and organ damage, which, in severe cases, can lead to multiple organ dysfunction (MODS) [7-9]. At the same time, a large amount of fluid loss in the blood vessels leads to shock [10,11].

At present, the mechanism of an increased endothelial cell permeability is still unclear, and effective clinical methods for treating capillary leakage are still lacking. In recent years, mining and identifying hub genes through genome sequencing technology and bioinformatic algorithms has become a method for exploring pathogenesis [12]. In this study, we identified the high-throughput sequencing expression profile of endothelial cell permeability-related genes from the Gene Expression Omnibus (GEO) database, conducted Gene Ontology (GO) and Kyoto Encyclopedia of Genes and Genomes (KEGG) enrichment analysis on differential genes, constructed a protein-protein interaction (PPI) network, and predicted related hub genes. Then, the hub gene associated with an increased endothelial cell permeability was confirmed through experiments, and its mechanism was elucidated by using molecular bioinformatics.

MATERIALS AND METHODS

Retrieval of data sets from the GEO database

In this study, the gene sequencing data with the keyword "endothelial cell permeability" were retrieved from the GEO database (https://www.ncbi.nlm.nih.gov/geo/). Thus, the gene high-throughput sequencing expression profile GSE178331, which met the requirements (including gene sequencing data of experimental and control cells), was downloaded. A total of 25 samples were included, of which 5 were normal control samples and the rest were experimental samples.

Screening of differentially expressed genes

The mRNA-Seq data were downloaded from the GEO database, and the probe ID was converted into a gene symbol. Data were divided into the experimental group and the control group, according to the limma package in the R software (Version 4.0.2). The logarithmic ratio changes (logFC), the p-value, and the correction p-values were calculated. Then, $p < 0.05$ and $|logFC| > 1$ were set as the inclusion criteria for the differentially expressed mRNA. Thus, differentially expressed genes were screened and heat maps were drawn.

GO/KEGG enrichment analysis

To further predict the biological functions and signaling pathways of the differential genes involved in an increased endothelial cell permeability, the GO functions and KEGG database were analyzed based on $p < 0.05$ by org.Hs/eg.db, ggplot2, and cluster Profiler in R.

Protein interaction analysis in the STRING database

The differential genes were utilized to produce a PPI network based on the Search Tool for the Retrieval of Interacting Genes/Proteins (STRING) database (https://string-db.org/), with a 0.4 confidence score and "Homo sapiens" setting. The visualizations and the data were downloaded to further screen out the hub genes.

Screening of network hub genes

The TSV format data, downloaded from the STRING database and the differential gene, were read into R language for visualization graphics.

Determination of endothelial cell permeability

Human umbilical vein endothelial cells (HUVECs) were obtained from the Cell Culture Center of the Chinese Academy of Medical Sciences. ECs were cultured in Dulbecco's Modified Eagle Medium (DMEM) supplemented with 10% fetal bovine serum (FBS), 100 μg/mL streptomycin, and 100 μg/mL penicillin, at 37°C in a fully humidified incubator with 5% CO_2. Cell viability was determined by trypan blue exclusion under experimental conditions. When grown to sub-confluence, the EC experiments were performed. FITC-labeled glucan (FD40) was used to evaluate the permeability of monolayer ECs. The ECs were inoculated on polycarbonate membrane (1×10^5) in Corning Costar (USA). Then, 100 μL DMEM medium containing FBS was added and cultured in a CO_2 incubator for 24 hours to form monolayer cells. Subsequently, the ECs were cultured in serum-free DMEM medium for 2 hours and were then replaced with fresh DMEM medium containing FBS. ECs were divided into three groups: high-dose TNF-α group, low-dose TNF-α group, and control group, with six well cells in each group. The ECs were then exposed to different TNF-α concentrations (10, 20 μg/L) in DMEM with 10% FBS diluted in the culture medium for 24 hours, or 100 μL phosphate buffer (PBS) was added for 24 hours under the same conditions. After stimulation, the ECs were washed twice with PBS. Subsequently, 100 μL of FITC-labeled glucan was added into the upper chamber and 600 μL of PBS was added into the lower chamber. After incubation at 37°C for 1 hour, the absorbance (A) values of the lower chamber were detected at a 490 nm wavelength. The experiment was repeated three times.

Table 1. Primers used for the quantitative RT-PCR.

Gene symbol	Primer	Sequence (5'-3')	TM	Length
GAPDH	Forward	GACCTGACCTGCCGTCTA	69°	18bp
	Reverse	AGGAGTGGGTGTCGCTGT	69°	18bp
ICAM1	Forward	GCAAGAAGATAGCCAACCAA	66°	20bp
	Reverse	TGCCAGTTCCACCCGTTC	66°	18bp
PTGS2	Forward	CTTGGGTGTCAAAGGTAAA	67°	19bp
	Reverse	ACTGATGCGTGAAGTGCTG	67°	19bp
SNAI1	Forward	TTACCTTCCAGCAGCCCTAC	71°	20bp
	Reverse	AGCCTTTCCCACTGTCCTC	71°	19bp

Total mRNA extraction and RT-PCR

ECs were cultured in 96-well plates with cell concentration of 5×10^3 per well. Cells were cultured overnight in an incubator containing 5% CO_2 at 37°C. The grouping and experimental methods for ECs were the same as described in section 3.1. The total mRNA of each group was extracted by using the Trizol reagent, and cDNA was reverse-transcribed by using the Prime Script II 1st Strand cDNA Synthesis Kit. The real-time PCR detection system and SYBR dye were applied to the PCR-amplified hub genes by following the manufacturer's instructions. The promoter primer sequence of the hub genes is shown in Table 1. Glyceraldehyde 3-phosphate dehydrogenase (GAPDH) was used as an internal reference. Relative expression of mRNA was calculated by using the $2^{-\Delta\Delta CT}$ method. The above-mentioned experiments were repeated three times each.

Protein extraction and western blot

The grouping and experimental methods for ECs were the same as explained in section 3.1. The total protein of ECs in the above-mentioned groups was extracted with RIPA lysis buffer, and the protein content was quantified with a BCA protein assay kit. The same amount of protein was then isolated by sodium dodecyl sulfate-polyacrylamide gel electrophoresis (SDS-PAGE) method and transferred to the polyvinylidene fluoride (PVDF) membrane. After blocking in 0.01% Tween 20 containing 5% skimmed milk powder for 4 hours, the membranes were incubated overnight with primary antibodies (ICAM-1, PTGS2, SANI1, and GAPDH) at a 1:800 dilution. The membranes were then incubated with anti-rabbit IgG secondary antibodies for 1 hour. Blot bands were visualized and quantified by a gel imaging system.

Statistical analysis

The one-way variance of analysis (ANOVA) was used for quantitative data, and a p-value less than 0.05 was considered a significant difference. Statistical tests were performed by using the SPSS version 19.0 statistical software package (IBM Corp., Armonk, NY, USA).

RESULTS

Differentially expressed genes

High-throughput mRNA sequencing data of ECs cultured *in vitro* stimulated by plasma from patients with COVID-19 were downloaded from GEO, a public database. A total of 19,480 genes were included, containing 6 normal control samples and 5 EC samples treated with serum from patients with a severe COVID-19 infection. After reading them into R language, FDR = 0.05 and logFC = 2 were set as inclusion criteria. It was calculated that there were 1,475 differentially expressed genes, including 1,224 up-regulated genes and 251 down-regulated genes, and the differential genes are visualized in Figure 1.

GO/KEGG analysis of differential genes

As shown in Figure 2, GO enrichment analysis of differential genes was conducted by using the Cluster Profiler in R language. Biological processes (BP), including laminar flow shear stress, tumor necrosis factor-alpha, cell membrane potential, negative regulation of endogenous apoptotic signaling pathway, adhesion connective tissue, and intercellular adhesion through serous membrane adhesion molecules, cellular component (CC), including golgi cis cisterna, collagen-extracellular matrix, and cationic channel complex, and molecular function (MF), including DNA binding transcription activity, RNA polymerase II specificity, cationic channel activity, metal ion transmembrane transporter activity, ion channel activity, channel activity, and passive transmembrane transporter activity, were obtained. Biological information with $p < 0.05$ is shown in Figure 2 (the top nine genes with $p < 0.05$ were selected). Moreover, KEGG enrichment analysis revealed that differential genes were mainly related to tumor necrosis factor receptor signaling pathways and laminar shear stress (Figure 3).

Screening of core genes

The protein interaction network diagram of differential genes (Figure 4), and the visualization of the arrange-

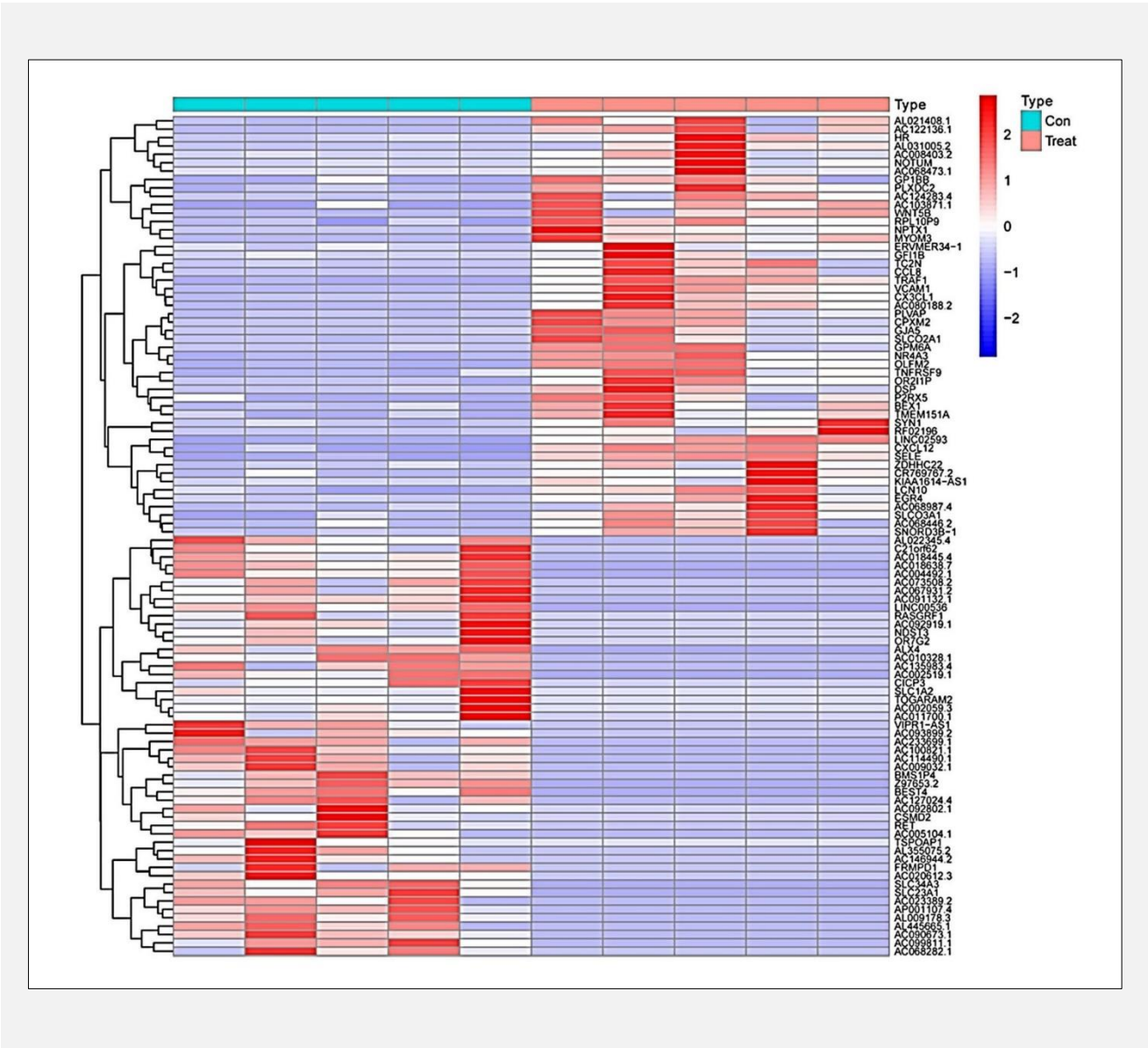

Figure 1. Heat map of differential genes.

The differential genes are represented by different colors. The redder the color, the more significant is the p-value, whereas the bluer the color, the less significant is the p-value.

ment according to the degree of freedom value of each differential gene (Figure 5), were obtained by using the STRING database and R language, respectively. As shown in Figure 5, the top three hub genes were PTGS2, ICAM1, and SNAI1.

Detection of EC permeability

The absorbance value (A) of the lower chamber stimulated by TNF-α (10 μg/L) was significantly different from that of the control group ($p = 0.02$, Table 1).

As the dose increased, the permeability gradually increased, and there was a statistically significant difference compared to the control group ($p = 0.008$, Figure 6A). This indicated that the selection of the dose and the time of TNF-α in this experiment was appropriate and proved that the model of an increased permeability of vascular ECs was successful.

mRNA and protein expression of the hub genes by TNF-α

To investigate the relationship between increased EC permeability and the hub genes predicted by the GEO network, the mRNA levels of PTGS2, ICAM1, and SNAI1 were measured by using quantitative real-time

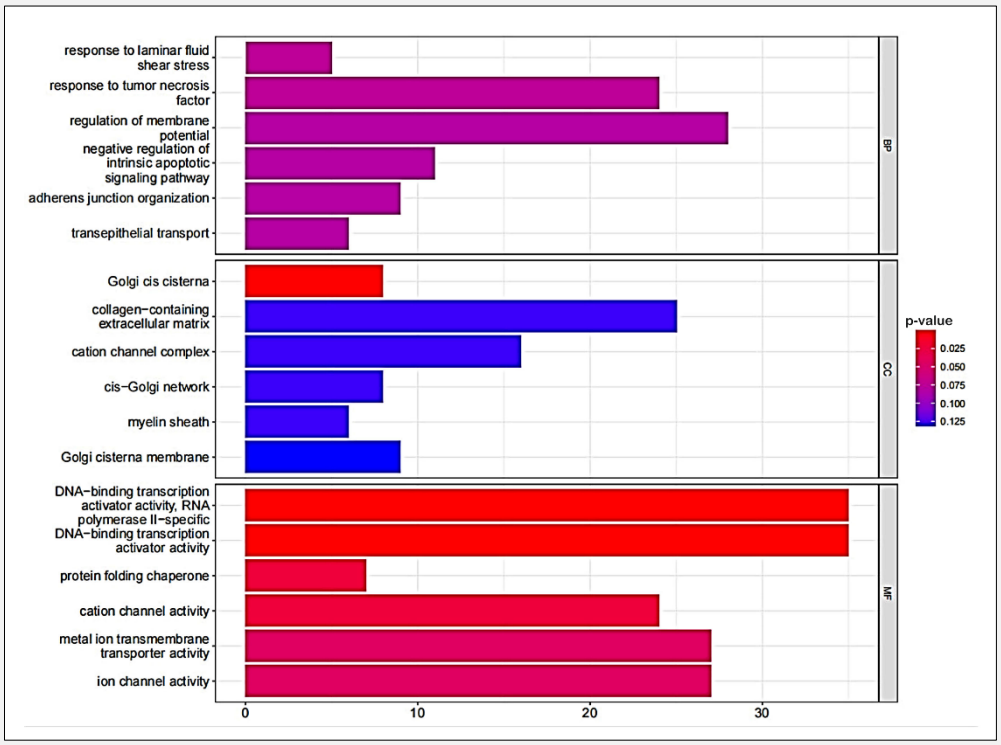

Figure 2. GO enrichment analysis of differential genes in R.

The differential genes are represented by columns of different colors. The redder the column color, the more significant is the p-value, whereas the bluer the column color, the less significant is the p-value.

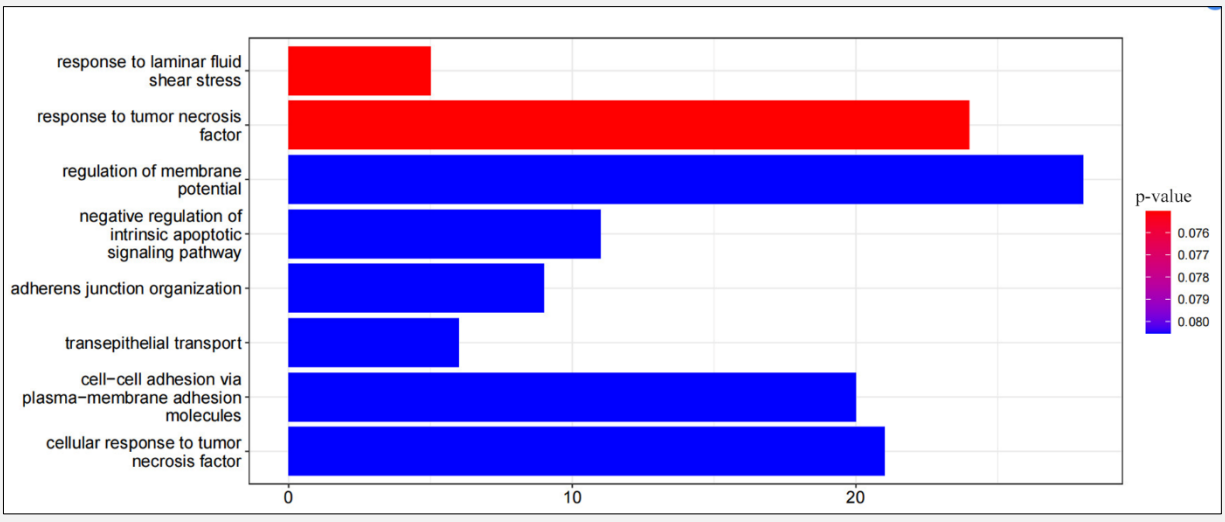

Figure 3. KEGG enrichment analysis of differential genes in R.

The differential genes are represented by columns of different colors. The redder the column color, the more significant is the p-value, whereas the bluer the column color, the less significant is the p-value.

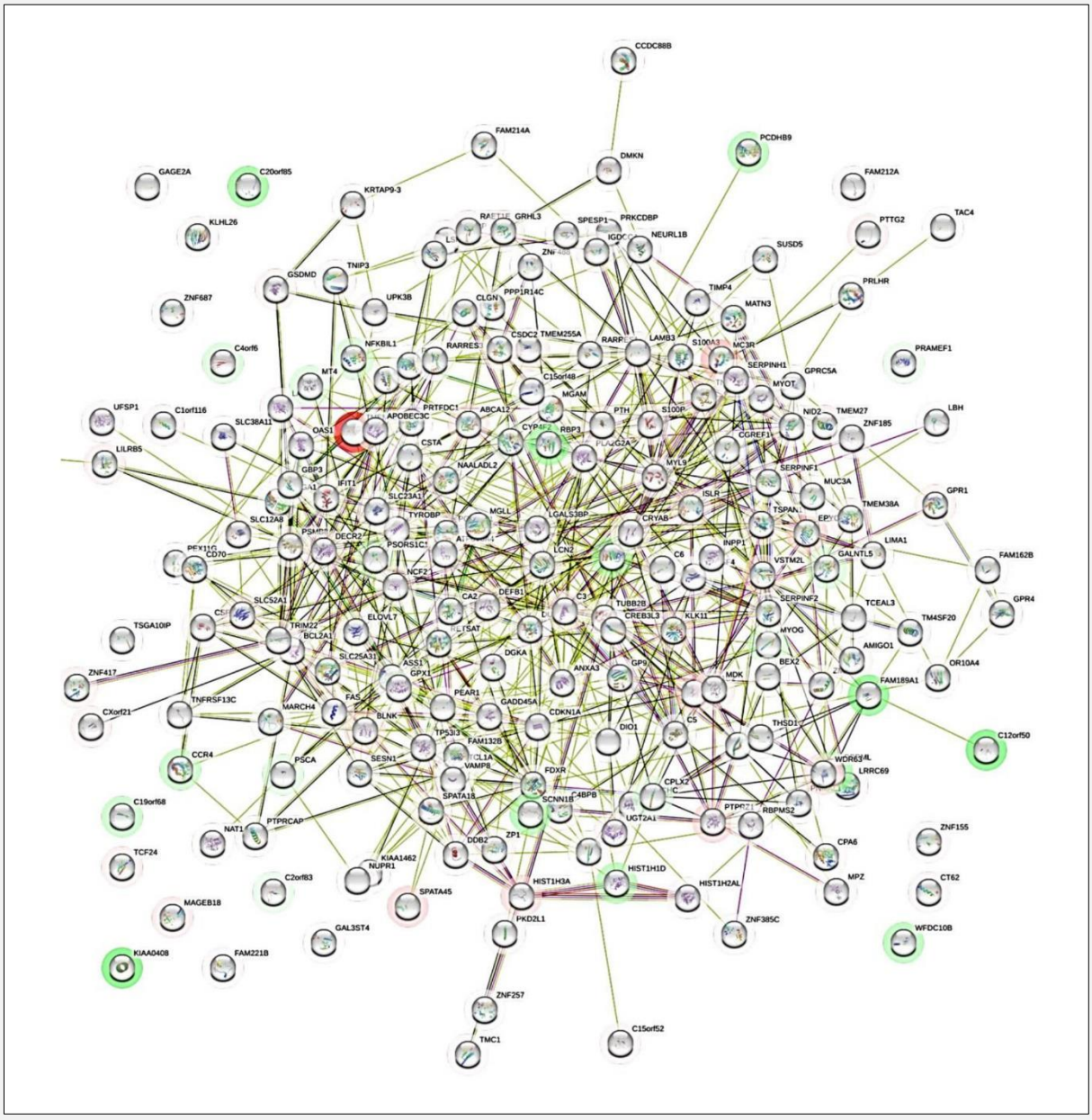

Figure 4. PPI for the differential genes.

Nodes are represented by circles of different colors. The darker the color, the higher the degree value, which indicates a stronger PPI. The edge indicates the correlation between the differential genes, and the thicker the edge, the closer is the correlation.

PCR, while the protein levels of PTGS2, ICAM1, and SNAI1 were measured by using western blot analysis. As shown in Figure 6B, the mRNA expressions of PTGS2, ICAM1, and SNAI1 were significantly increased after TNF-α stimulation, which was dose-dependent. In addition, the protein expressions of PTGS2, ICAM1, and SNAI1 were significantly increased by TNF-α, showing a dose-dependent relationship (Figure 7). Collectively, the results of our study confirm that PTGS2, ICAM1, and SNAI1 are hub genes of EC permeability increase, as predicted by the GEO network.

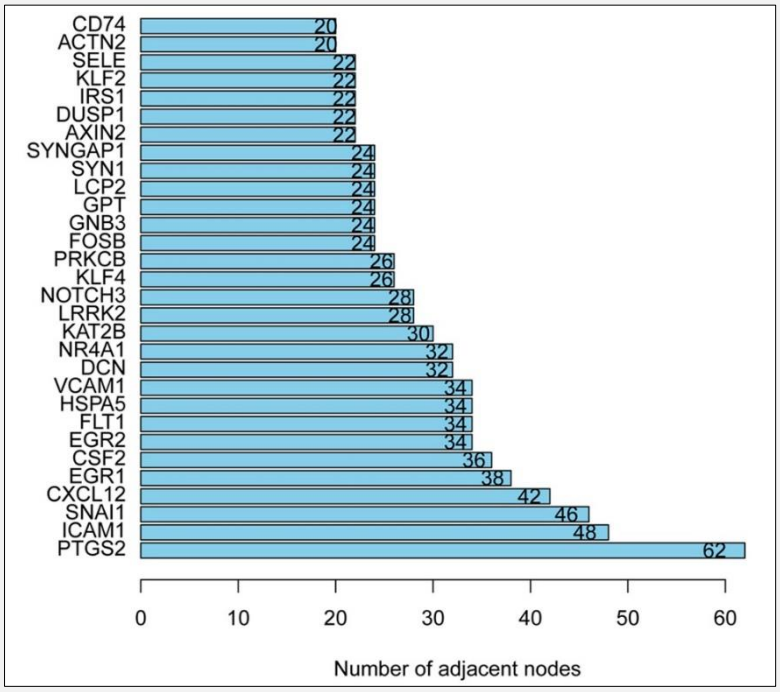

Figure 4. PPI for the differential genes.

Nodes are represented by circles of different colors. The darker the color, the higher the degree value, which indicates a stronger PPI. The edge indicates the correlation between the differential genes, and the thicker the edge, the closer is the correlation.

DISCUSSION

Capillary leakage is a common clinical symptom caused by a wide range of inflammatory diseases [5,6,11]. EC permeability increase is the basis of capillary leakage [8,9]. When ECs are stimulated by inflammatory cytokines, they get activated and the integrity of the EC barrier function is destroyed. At this time, the permeability of ECs increases, and then the macromolecules in the blood vessels that normally cannot be penetrated leak out of the blood vessels, leading to the occurrence of capillary leakage [13-16]. TNF-α is a major proinflammatory cytokine, which can directly activate or damage ECs and lead to an increased permeability of ECs [17-20]. Our research is the first to elucidate the molecular mechanism of an increased EC permeability through data mining approaches from the GEO database and experimental studies, and with that lays the foundation for further clinical studies.

In this study, the keyword "endothelial cell permeability" was searched in the GEO public database, and the dataset GSE178331, which met the requirements (having an experimental group, control group, and sample content greater than six), was retrieved. We obtained 1,475 differentially expressed genes (DEGs) by using R language. Then, GO and KEGG enrichment analyses were performed by using R. GO function analysis showed that the DEGs were significantly enriched in laminar flow shear stress, TNF-α, adhesion junction, channel activity, and passive transmembrane transporter activity. KEGG enrichment analysis showed that the DEGs were significantly enriched in tumor necrosis factor receptor signaling pathway and laminar shear stress. These analyses suggest that TNF-α may be a key factor in the increase of EC permeability. The top three hub genes, namely PTGS2, ICAM1, and SNAI1, were selected through the topological property analysis of the PPI network and the value of degree by using R. PTGS2 (prostaglandin-endoperoxide synthase 2), also known as COX-2 (cyclooxygenase 2), is one of the targets of nonsteroidal drugs. When stimulated by inflammation, the expression level of COX-2 increases, leading to endothelial apoptosis and vascular endothelial injury [21,22]. ICAM-1 (intercellular cell adhesion moleculin-1) is constitutively present in ECs, but its expression is increased by proinflammatory cytokines. In addition to acting as a leukocyte adhesion molecule, ICAM-1 directly contributes to inflammatory responses within the blood vessel wall by increasing EC activation [23-27]. SNAI1, as a zinc finger protein, negatively regu-

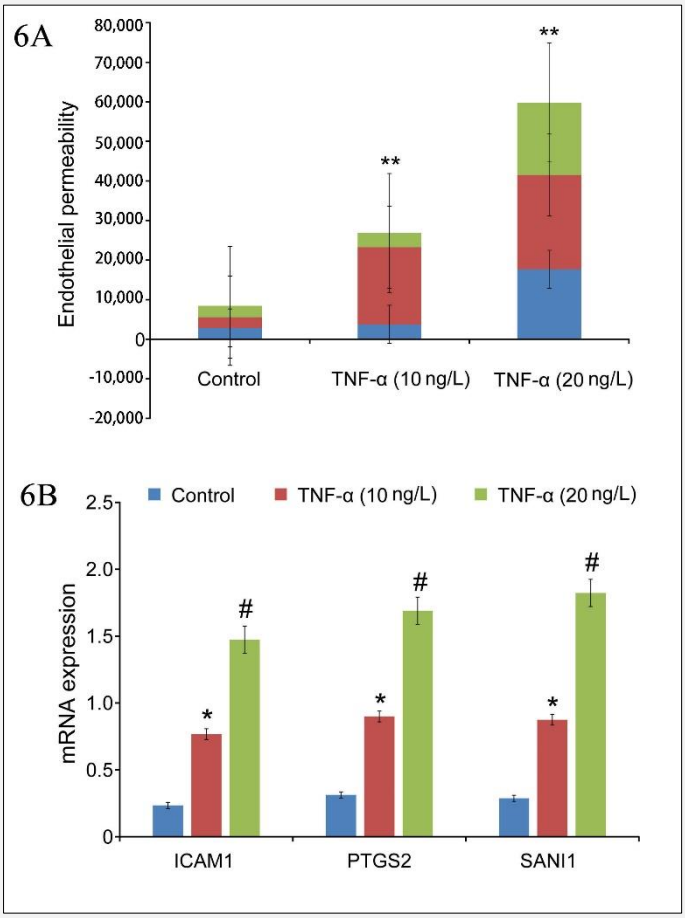

Figure 6.
6A: Effect of TNF-α on the endothelial permeability.
Data are presented as the mean ± SEM (n = 3); ** $p < 0.01$ versus control group was considered a statistically significant difference.
6B: Effect of TNF-α on the hub gene mRNA expression levels in ECs.
mRNA levels were determined by RT-PCR. Data are presented as the mean ± SEM (n = 3); * $p < 0.05$ and $^{\#}$ $p < 0.01$ versus control group were considered statistically significant differences.

lates the transcription of vascular endothelial-cadherin, when its expression is increased [28,29]. Moreover, when SNAI1 expression is upregulated, it can also promote endothelial mesenchymal transformation (EMT) [30]. These results suggest that the increased permeability of ECs may be due to these hub genes.

To verify the role of hub genes, as predicted above, in the increased EC permeability, a classical inflammation model was developed by using ECs stimulated by TNF-α, which was used to study the mechanism of the increased endothelial cell permeability [24-26]. The results showed that the permeability of ECs was significantly increased by TNF-α in a concentration-dependent manner ($p = 0.008$ vs. $p = 0.0004$). Moreover, RT-PCR validated mRNA expressions of PTGS2, ICAM1, and SNAI1, which differed significantly between the different TNF-α-induced and control groups ($p < 0.05$ vs. $p < 0.01$, respectively). The protein expression levels of the hub genes by western blot also differed significantly between the different TNF-α-induced and control groups ($p < 0.05$ vs. $p < 0.01$, respectively), suggesting that an increased permeability of ECs may be caused by the predicted hub genes.

Our study demonstrates significant strengths in identifying key genes responsible for an increased vascular endothelial cell permeability, particularly through the innovative combination of the GEO database and WGCNA. This approach enhances the accuracy and ef-

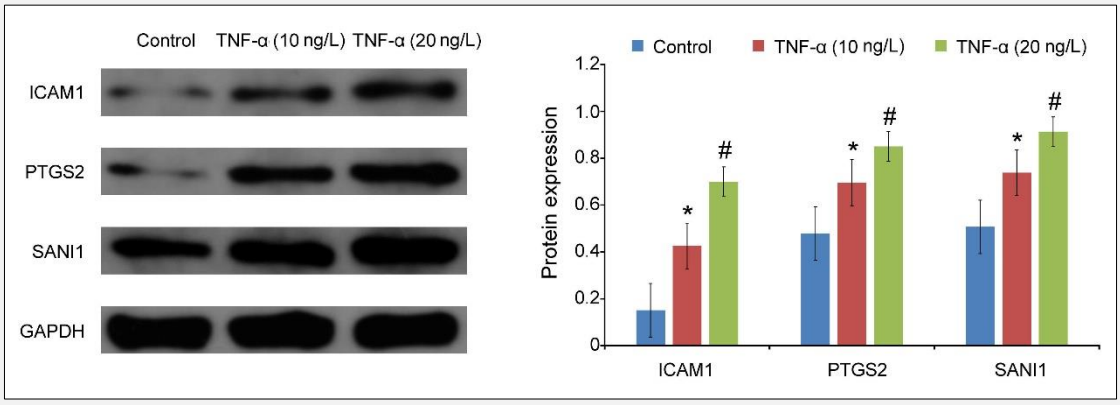

Figure 7. Effect of TNF-α on key protein expression levels in ECs.

The expression of PTGS2, ICAM1, and SNAI1 protein levels were determined by western blot with specific antibodies and quantification. Data are presented as the mean ± SEM (n = 3); * $p < 0.05$ and # $p < 0.01$ versus control group were considered statistically significant differences.

ficiency in key gene identification. The thoroughness of experimental validation, employing RT-PCR and Western Blot techniques to verify predictive outcomes, bolsters the study's credibility. The successful identification of three hub genes (PTGS2, ICAM1, and SNAI1) offers potential targets for future therapies, and the in-depth exploration of TNF-α's role in regulating endothelial cell permeability enriches our understanding of inflammation and vascular dysfunction.

However, our study is not without limitations. Primarily, it is limiting the sample scope. Future research should expand the sample size and variety to enhance the universality of the findings. Although the study reveals key genes, a comprehensive exploration of their mechanisms and impacts in various pathological states remains to be conducted. Additionally, while this research provides new directions for clinical treatment, the efficacy and safety of these findings in clinical applications require validation through extensive clinical trials. Lastly, gene co-expression network analysis, while a powerful tool, demands a high degree of expertise and experience for interpretation, possibly limiting the application and comprehension of the results in a broader scientific and medical context. Future research, therefore, needs to delve deeper into aspects like sample range, pathological mechanisms, clinical application, and the complexity of data interpretation.

CONCLUSION

In conclusion, the DEGs associated with an increased permeability of ECs were mined from the GEO database, and three hub genes, namely PTGS2, ICAM1, and SNAI1, were screened by PPI network topological properties and R. Then, an experimental *in vitro* validation was performed to confirm the mRNA and protein expression of these hub genes. The mechanism of an increased permeability of ECs may happen through the action of these hub genes.

Acknowledgment:
We would like to acknowledge the hard and dedicated work of all of the staff that implemented the intervention and evaluation components of the study.

Ethics Approval Statement:
This study was conducted with the approval from the Ethics Committee of the Chongming Hospital. This study was conducted in accordance with the Declaration of Helsinki.

Availability of Data and Materials:
The datasets used during this study are available from the corresponding author upon reasonable request.

Declaration of Interest:
The authors report no conflicts of interest. The authors alone are responsible for the content and writing of this article. There are no financial or personal relationships with other people or organizations that could have inappropriately influenced (biased) their work.

References:

1. Armstrong SM, Khajoee V, Wang C, et al. Co-regulation of transcellular and paracellular leak across microvascular endothelium by dynamin and Rac. Am J Pathol 2012;180:1308-23. (PMID: 22203054)

2. Xie Z, Ghosh CC, Patel R, et al. Vascular endothelial hyperpermeability induces the clinical symptoms of Clarkson disease (the systemic capillary leak syndrome). Blood 2012;119:4321-32. (PMID: 22411873)

3. Yang X, Meegan JE, Jannaway M, Coleman DC, Yuan SY. A disintegrin and metalloproteinase 15-mediated glycocalyx shedding contributes to vascular leakage during inflammation. Cardiovasc Res 2018;114(13):1752-63. (PMID: 29939250)

4. Korkmaz HI, Ulrich MMW, van Wieringen WN, et al. C1 Inhibitor Administration Reduces Local Inflammation and Capillary Leakage, Without Affecting Long-term Wound Healing Parameters, in a Pig Burn Wound Model. Antiinflamm Antiallergy Agents Med Chem 2021;20(2):150-60. (PMID: 32614753)

5. Joris I, Cuénoud HF, Doern GV, Underwood JM, Majno G. Capillary leakage in inflammation. A study by vascular labeling. Am J Pathol 1990;137(6):1353-63. (PMID: 2260625)

6. Schuerer-Maly CC, Ott K, Emmenegger U, Hoeflin F, Müller EO, Halter F. Inflammation, capillary leakage and healing of experimental gastric ulcers in the rat. Digestion 1991;50(3-4):170-5. (PMID: 1667393)

7. Duan C-Y, Zhang J, Wu H-L, Li T, Liu L-M. Regulatory mechanisms, prophylaxis and treatment of vascular leakage following severe trauma and shock. Mil Med Res 2017;4:11. (PMID: 28361006)

8. Marx G. Fluid therapy in sepsis with capillary leakage. Eur J Anaesthesiol 2003;20(6):429-42. (PMID: 12803259)

9. Bauer PR. Microvascular responses to sepsis: clinical significance. Pathophysiology 2002;8(3):141-8. (PMID: 12039645)

10. Etzrodt V, Idowu TO, Schenk H, et al. Role of endothelial microRNA 155 on capillary leakage in systemic inflammation. Crit Care 2021;25(1):76. (PMID: 33618730)

11. Li Z, Yin M, Zhang H, et al. BMX Represses Thrombin-PAR1-Mediated Endothelial Permeability and Vascular Leakage During Early Sepsis. Circ Res 2020;126(4):471-85. (PMID: 31910739)

12. Akalin PK. Introduction to bioinformatics. Mol Nutr Food Res 2006;50(7):610-9. (PMID: 16810733)

13. Pan X, Xu S, Zhou Z, et al. Fibroblast growth factor-2 alleviates the capillary leakage and inflammation in sepsis. Mol Med 2020; 26(1):108. (PMID: 33187467)

14. Hellenthal KEM, Brabenec L, Wagner N-M. Regulation and Dysregulation of Endothelial Permeability during Systemic Inflammation. Cells 2022;11(12):1935. (PMID: 35741064)

15. Asgharzadeh F, Barneh F, Fakhraie M, et al. Metformin inhibits polyphosphate-induced hyper-permeability and inflammation. Int Immunopharmacol 2021;99:107937. (PMID: 34271418)

16. Van Nguyen D, Nguyen TLL, Jin Y, Kim L, Myung C-S, Heo K-S. 6'-Sialylactose abolished lipopolysaccharide-induced inflammation and hyper-permeability in endothelial cells. Arch Pharm Res 2022;45(11):836-48. (PMID: 36401777)

17. Wang B, Chen R, Gao H, et al. A comparative study unraveling the effects of TNF-α stimulation on endothelial cells between 2D and 3D culture. Biomed Mater 2020;15(6):065018. (PMID: 32442992)

18. Fong LY, Ng CT, Yong YK, Hakim MN, Ahmad Z. Asiatic acid stabilizes cytoskeletal proteins and prevents TNF-α-induced disorganization of cell-cell junctions in human aortic endothelial cells. Vascul Pharmacol 2019;117:15-26. (PMID: 30114509)

19. Zuniga M, Gomes C, Chen Z, et al. Plasmodium falciparum and TNF-α Differentially Regulate Inflammatory and Barrier Integrity Pathways in Human Brain Endothelial Cells. mBio 2022;13(5): e0174622. (PMID: 36036514)

20. Marcos-Ramiro B, García-Weber D, Millán J. TNF-induced endothelial barrier disruption: beyond actin and Rho. Thromb Haemost 2014;112(6):1088-102. (PMID: 25078148)

21. Wang Z, Liu P, Hu M, et al. Naoxintong restores ischemia injury and inhibits thrombosis via COX2-VEGF/ NFκB signaling. J Ethnopharmacol 2021;270:113809. (PMID: 33444716)

22. Shao J, Ding J, Lu L, et al. Propofol protects against high glucose-mediated endothelial injury via inhibition of COX2 and iNOS expressions. Acta Biochim Biophys Sin (Shanghai) 2022; 54(4):548-55. (PMID: 35607962)

23. Lawson C, Wolf S. ICAM-1 signaling in endothelial cells. Pharmacol Rep 2009;61(1):22-32. (PMID: 19307690)

24. Zhang Y, Zhang L, Zheng S, et al. Fusobacterium nucleatum promotes colorectal cancer cells adhesion to endothelial cells and facilitates extravasation and metastasis by inducing ALPK1/NF-κB/ICAM1 axis. Gut Microbes 2022;14(1):2038852. (PMID: 35220887)

25. Beddek K, Raffin F, Borgel D, et al. TRPV4 channel activation induces the transition of venous and arterial endothelial cells toward a pro-inflammatory phenotype. Physiol Rep 2021;9(3): e14613. (PMID: 33512067)

26. Bian Z, Liu H, Xu F, Du Y. Ursolic acid protects against anoxic injury in cardiac microvascular endothelial cells by regulating intercellular adhesion molecule-1 and toll-like receptor 4/MyD88/ NF-κB pathway. Hum Exp Toxicol 2022;41: 9603271221093626. (PMID: 35438581)

27. Gu W, Zhang L, Zhang X, et al. MiR-15p-5p Mediates the Coordination of ICAM-1 and FAK to Promote Endothelial Cell Proliferation and Migration. Inflammation 2022;45(3):1402-17. (PMID: 35079920)

28. Gao P, Tian Y, Xie Q, Zhang L, Yan Y, Xu D. Manganese exposure induces permeability in renal glomerular endothelial cells via the Smad2/3-Snail-VE-cadherin axis. Toxicol Res (Camb) 2020;9(5):683-92. (PMID: 33178429)

29. Zheng Y-J, Zhou B, Ding G, et al. Effect of serum from patients with severe acute pancreatitis on vascular endothelial permeability. Pancreas 2013;42(4):633-9. (PMID: 23303203)

30. Chandran Latha K, Sreekumar A, Beena V, et al. Shear Stress Alterations Activate BMP4/pSMAD5 Signaling and Induce Endothelial Mesenchymal Transition in Varicose Veins. Cells 2021; 10(12):3563. (PMID: 34944071)